

LOW ENERGY E0 TRANSITIONS IN ODD-MASS NUCLEI OF THE NEUTRON DEFICIENT 180<A<200 REGION\*

E. F. Zganjar and M. O. Kortelahti  
Department of Physics and Astronomy  
Louisiana State University, Baton Rouge, LA 70803, USA

J. L. Wood and C. D. Papanicolopoulos  
School of Physics  
Georgia Institute of Technology, Atlanta, GA 30332, USA

ABSTRACT

The region of neutron-deficient nuclei near Z=82 and N=104 provides the most extensive example of low-energy shape coexistence anywhere on the mass surface. It is shown that E0 and E0 admixed transitions may be used as a fingerprint to identify shape coexistence in odd-mass nuclei. It is also shown that all the known cases of low energy E0 and E0 admixed transitions in odd-mass nuclei occur where equally low-lying 0+ states occur in neighboring even-even nuclei. A discussion of these and other relevant data as well as suggestions for new studies which may help to clarify and, more importantly, quantify the connection between E0 transitions and shape coexistence are presented.

INTRODUCTION

Nuclei in the far from stability region between  $78 \leq Z \leq 83$  and  $104 \leq N \leq 109$  have been discussed by many authors (see e.g. refs. 1, 2) as the most extensive region known exhibiting coexisting nuclear shapes. We reported earlier on the observation in  $^{185,187}\text{Au}$  ( $Z=79$ ;  $N=106, 108$ ) of a systematic pattern of bands interconnected with low-energy very converted transitions<sup>3,4</sup>. In contrast to other reports (e.g. ref. 5) which indicated that the very converted cases were anomalous M1 transitions, we have clearly shown that these very converted transitions are entirely consistent with an E0 multipole component and that they closely match low-energy E0 transitions in the neighboring doubly-even isotopes. This is shown in fig. 1 for the case of  $^{185}\text{Au}$ . The systematic pattern of transitions with E0 components in  $^{185}\text{Au}$  (and  $^{187}\text{Au}$ , see ref. 4) bears a close resemblance to E0 and E0 admixed transitions in the neighboring doubly-even Pt and Hg isotopes which are considered cores for certain configurations in the odd-mass Au isotopes. The relevant Hg and Pt cores are shown in fig. 2; and the corresponding conversion coefficients are given in Table I.

The  $9/2^-$  state at 9 keV (see fig. 1) is the proton  $h_{9/2}$  particle (intruder) state. The particle character has the consequence that the appropriate core for this configuration in  $^{185}\text{Au}$  is  $^{184}\text{Pt}$ . The  $11/2^-$  state at 220 keV is the proton  $h_{11/2}$  hole state. The appropriate core for proton hole configurations in  $^{185}\text{Au}$  is  $^{186}\text{Hg}$ .

\*Work supported in part by DOE grant DE-FG05-84ER40159 (LSU), DE-FG05-87ER40330 (Ga. Tech.), and DOE contract DE-AC05-76OR00033 (UNISOR).

MASTER

DISTRIBUTION OF THIS DOCUMENT IS UNLIMITED

The submitted manuscript has been authored by a contractor of the U. S. Government under Contract No. DE-AC05-76OR00033. Accordingly, the U. S. Government retains a nonexclusive, royalty-free license to publish or reproduce the published form of this contribution, or allow others to do so for U. S. Government purposes.

The submitted manuscript has been authored by a contractor of the U.S. Government under contract No. DE-AC05-84OR21400. Accordingly, the U.S. Government retains a nonexclusive, royalty-free license to publish or reproduce the published form of this contribution, or allow others to do so, for U.S. Government purposes.

## **DISCLAIMER**

This report was prepared as an account of work sponsored by an agency of the United States Government. Neither the United States Government nor any agency thereof, nor any of their employees, makes any warranty, express or implied, or assumes any legal liability or responsibility for the accuracy, completeness, or usefulness of any information, apparatus, product, or process disclosed, or represents that its use would not infringe privately owned rights. Reference herein to any specific commercial product, process, or service by trade name, trademark, manufacturer, or otherwise does not necessarily constitute or imply its endorsement, recommendation, or favoring by the United States Government or any agency thereof. The views and opinions of authors expressed herein do not necessarily state or reflect those of the United States Government or any agency thereof.

WV2LEB  
SET2AM

See refs. 6, 7 for a discussion of the coupling of these configurations to Pt and Hg cores for the case of  $^{185}\text{Au}$ . The association between  $^{185}\text{Au}$  states and  $^{184}\text{Pt}$ ,  $^{186}\text{Hg}$  states, shown in fig. 1 by dashed lines, is suggested as reflecting the major components of the particle- and hole-coupled wave functions. Such a pattern of bands connected by low-energy transitions with E0 components is suggested to reflect a new type of particle-core coupling in nuclei.

Early in-beam  $\gamma$ -ray spectroscopy on  $^{184,186}\text{Hg}$  showed that their yrast bands become deformed above the  $2^+$  state<sup>8,9</sup> and studies of the decay of  $^{188,186,184}\text{Tl} \rightarrow ^{188,186,184}\text{Hg}$  at UNISOR and ISOCELE clearly revealed two coexisting bands which approach each other with decreasing neutron number<sup>10-14</sup>. Not shown in fig. 2 is  $^{184}\text{Hg}$  where the  $0^+$  is at 375 keV<sup>11</sup>. In-beam work<sup>15</sup> on  $^{182}\text{Hg}(N=102)$  indicates that the deformed configuration in that nucleus is nearing a minimum at the mid neutron shell ( $N=104$ ) as one would expect based on a microscopic model<sup>16-18</sup> which incorporates an explicit dependence on proton and neutron number through a proton-neutron force. These Hg data provide a classic example of the coexistence of levels built on different shapes in even-even nuclei. More recently excited  $0^+$  deformed states have been observed<sup>19</sup> in the neutron deficient, closed shell,  $Z=82$ , Pb isotopes  $^{190-198}\text{Pb}$ . These  $0^+$  configurations also exhibit a continuous drop in energy with decreasing mass as one approaches  $N=104$  such that the deformed  $0^+$  even becomes the first excited state in  $^{190-194}\text{Pb}$ .<sup>19</sup>

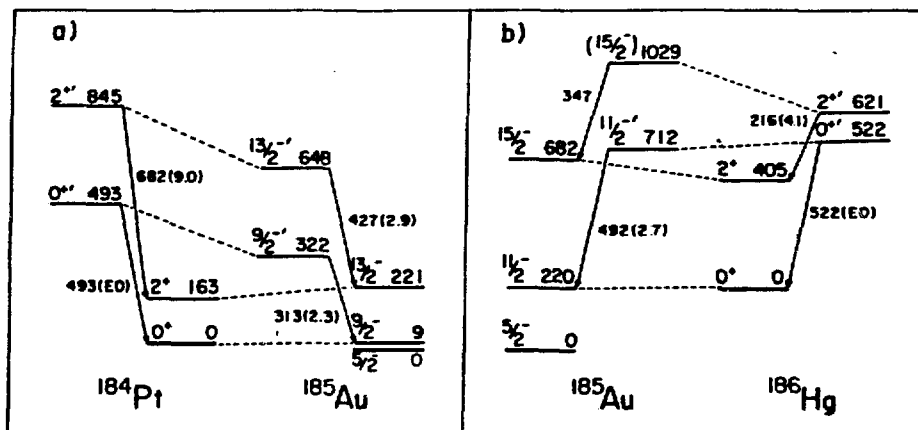


Fig. 1. Part a): Portions of the  $h_{9/2}$  and  $h_{7/2}$  bands in  $^{185}\text{Au}$  compared to the  $0^+$  and  $0^+$  bands in  $^{184}\text{Pt}$ . Part b): Portions of the  $h_{11/2}$  and  $h_{7/2}$  bands in  $^{185}\text{Au}$  compared to the  $0^+$  and  $0^+$  bands in  $^{186}\text{Hg}$ . Only transitions with  $\alpha_K > \alpha_K(M1)$  are shown. All energies are in KeV. The numbers in parentheses following the transition energy are the ratios  $\alpha_K(\text{expt})/\alpha_K(M1 \text{ theory})$  for transitions where  $I \neq 0$ . The data are from refs. 3, 4, and 20. The  $^{185}\text{m}, ^{185}\text{g}\text{Hg}$  decay contains three 347 keV transitions and thus a multipolarity for the 1029 keV  $\rightarrow$  682 keV 347 keV transition (part b) could not be determined.

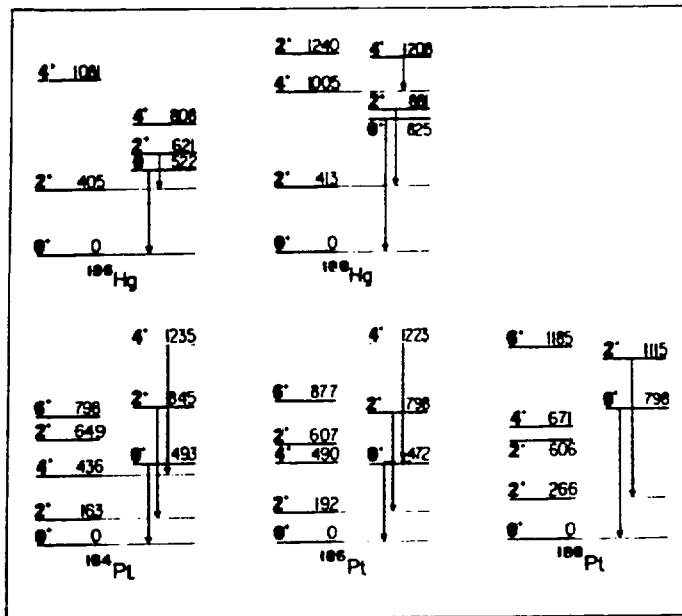


Fig. 2. Systematics of the low-lying levels in  $^{186,188}\text{Hg}$ ,  $^{184,186,188}\text{Pt}$ . Transitions which are pure E0 or with E0 admixtures are indicated. Data are from refs. 21( $^{184}\text{Pt}$ ), 13( $^{186}\text{Hg}$ ), 22( $^{186,188}\text{Pt}$ ), and 14( $^{188}\text{Hg}$ ).

Table I. K-conversion coefficients for the  $I_i^{\pi} \rightarrow I_f^{\pi}$  ( $I \neq 0$ ) transitions in the Hg and Pt isotopes shown in fig. 2.

Isotope	$E_{\gamma}$ (keV)	$E_i$ (keV)	$I_i^{\pi}$	Experiment		Theory <sup>23</sup>	
				$\alpha_K$	ref.	$\alpha_K(\text{M1})$	$\alpha_K(\text{E2})$
$^{186}\text{Hg}$	216	621	$2^+$	3.1 (7)	13	0.76	0.14
$^{188}\text{Hg}$	468	881	$2^+$	0.087 (6)	14	0.093	0.022
	203	1208	$4^+$	0.99 (11)	14	0.89	0.16
$^{184}\text{Pt}$	682	845	$2^+$	0.28 (6)	21	0.031	0.010
	799	1235	$4^+$	0.049 (10)	21	0.020	0.0074
$^{186}\text{Pt}$	606	798	$2^+$	>0.10*	22	0.041	0.013
	733	1223	$4^+$	0.057 (22)	22	0.025	0.0091
$^{188}\text{Pt}$	849	1115	$2^+$	0.22 (1)	22	0.016	0.0067

\*Doublet. Lower limit computed from  $I_K/I_{\gamma}$  given in ref. 22. The other component is probably E2.

## DISCUSSION

Low-energy transitions with E0 components between states with  $I^{\pi} \neq 0^+$  are fairly common in doubly-even nuclei. However, in odd-mass nuclei, low-energy transitions with E0 components are very rare; and

even relaxing the low-energy criterion, they are still uncommon. In Table II we list (in increasing order by energy) all the cases known to us in odd-mass nuclei of low-energy transitions ( $E < 430$  keV) with EO components. While it is surprising that only 16 cases below 430 keV are known, one immediately notes that 13 of the 16 cases are odd-mass neighbors of the even-even nuclei listed in Table I. Low-lying ( $< 600$  keV) excited  $0^+$  states are not commonly known in nuclei. We list all the cases known to us in Table III. Note that all the isotopes listed in Table II are odd-mass neighbors of even-even nuclei listed in Table III. Table III can be used to suggest other odd-mass candidates for low-energy EO admixed transitions.

Table II. The lowest-energy transitions with EO components known between low-lying levels in odd-mass nuclei. All known cases with  $E_\gamma \leq 430$  keV are shown.

Isotope	$E_\gamma$ (keV)	$E_i$ (keV)	$I_i^\pi$	ref.
$^{185}\text{Au}$	205	497	$5/2^+$	24,25
$^{187}\text{Pt}$	260	260	$3/2^-$	26,27
$^{187}\text{Pt}$	262	288	$5/2^-$	26,27
$^{185}\text{Au}$	281	515	$5/2^+$	24
$^{183}\text{Au}$	284	----not certain----	----	28
$^{185}\text{Au}$	289	289	$5/2^-$	24
$^{183}\text{Au}$	297	----not certain----	----	28
$^{185}\text{Au}$	313	322	$9/2^-$	3,4,24
$^{195}\text{Pb}$	318	1126	$11/2^+$	29
$^{187}\text{Au}$	323	444	$9/2^-$	30,33
$^{185}\text{Au}$	330	371	$3/2^+$	24,25
$^{185}\text{Pt}$	340	521	$3/2^-$	31
$^{187}\text{Au}$	388	742	$13/2^-$	30,33
$^{195}\text{Pb}$	401	1177	$9/2^+$	29
$^{185}\text{Au}$	427	648	$13/2^-$	3,4,24
$^{231}\text{Th}$	429	634	$7/2^-$	32

The unique occurrence of EO and EO admixed low-energy transitions in both even- and odd-mass nuclei for  $78 \leq Z \leq 80$  and  $104 \leq N \leq 109$ , together with the systematic features<sup>20</sup> for  $^{185}, ^{187}\text{Au}$  observed at UNISOR, leads us to propose a new type of multiple band structure in odd-mass nuclei (fig. 1 for  $^{185}\text{Au}$ ). The essential features are: two bands interconnected by transitions with strong EO components, a small ( $< 500$  keV) energy separation between the bands, and the absence of well-defined strong coupling in the bands.

Pairs of bands interconnected by transitions with intense EO admixtures are known in strongly-deformed odd-mass nuclei. Some examples of note are  $^{231}\text{Th}$  (ref. 32),  $^{155}\text{Eu}$  (ref. 41), and  $^{173}\text{Lu}$  (ref. 42). The systematic occurrence of such pairs has also been reported<sup>43</sup> in the actinides. An example for  $^{235}\text{U}$  is presented in fig. 3. To our knowledge, however, the present work reports the first systematic occurrence of pairs of bands interconnected by

Table III. The lowest first excited  $0^+$  states known in doubly-even nuclei. All known cases with  $E_x \leq 635$  keV are shown.

Isotope	$E_x$	ref.	comments
$^{98}\text{Sr}$	215	34	
$^{100}\text{Zr}$	331	35	
$^{184}\text{Hg}$	375	11,36	
$^{178}\text{Pt}$	(422)	39	$0^+$ spin inferred
$^{176}\text{Pt}$	(433)	39	$0^+$ spin inferred
$^{186}\text{Pt}$	472	22	
$^{184}\text{Pt}$	492	21	
$^{182}\text{Pt}$	500	40	
$^{180}\text{Pt}$	(500)	-	estimate from systematics
$^{186}\text{Hg}$	522	13	
$^{152}\text{Gd}$	615	37	
$^{230}\text{Th}$	635	38	

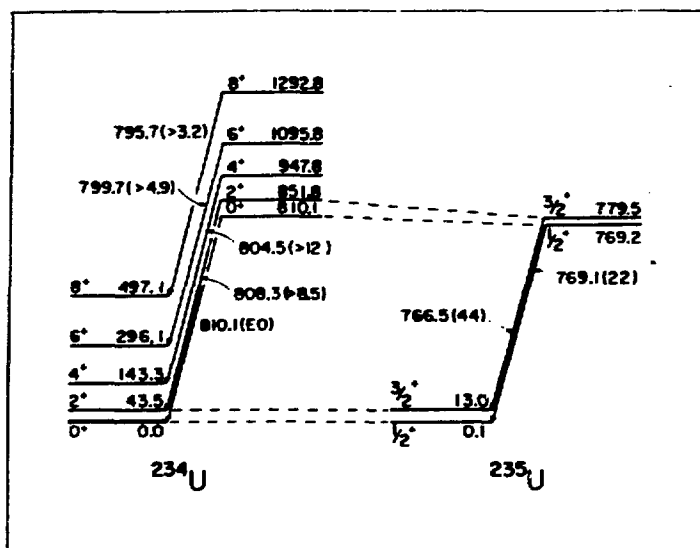


Fig. 3. Comparison of the ground state and  $\alpha$ -bands in  $^{234}\text{U}$  and  $^{235}\text{U}$ . All energies are in keV. Only transitions with  $\alpha_K > \alpha_K(\text{M1})$  are shown. The numbers in parentheses following the transition energy are the ratios  $\alpha_K(\text{expt})/\alpha_K(\text{M1 theory})$  for transitions where  $I \neq 0$ . The  $^{235}\text{U}$  ground state is  $7/2^-$  and the basic configuration of the bands is  $[631+]$ . The data are from refs. 44( $^{234}\text{U}$ ) and 45( $^{235}\text{U}$ ).

transitions with intense E0 admixtures outside of the traditional strongly-deformed regions, and it is significantly lower in energy.

K-conversion coefficients for  $I_i^\pi \rightarrow I_f^\pi$  transitions with E0 components for the cases given in Table II and, for completeness, the additional transitions with energy > 430 keV, which will be needed for the remaining figures, are presented in Table IV. Obvious missing entries include Hg and Tl isotopes. Data for  $^{189,193}\text{Hg}$  (ref. 46)  $^{195}\text{Hg}$  (ref. 47) and  $^{197}\text{Hg}$  (ref. 48) are either preliminary or the transitions are much higher in energy. Studies on  $^{193,195}\text{Tl}$  are underway (ref. 49).

**Table IV.** K-conversion coefficients for  $I_i^\pi \rightarrow I_f^\pi$  transitions with E0 components for the cases given in Table II and, for completeness, the additional transitions with energy >430 keV.

Isotope	$E_\gamma$ (keV)	$E_i$ (keV)	$I_i^\pi$	Experiment		Theory <sup>23</sup>	
				$\alpha_K$	ref.	$\alpha_K$ (M1)	$\alpha_K$ (E2)
$^{183}\text{Au}$	284	-not certain-		1.6	28	0.33	0.069
	297	-not certain-		3.9	28	0.28	0.064
$^{185}\text{Au}$	205	497	$5/2^+$	2.5 (5)	24,25	0.82	0.16
	281	515	$5/2^+$	0.77 (41)	24	0.34	0.073
	289	289	$5/2^-$	0.52 (20)	24	0.32	0.068
	313	322	$9/2^-$	0.58 (15)	3,4,24	0.26	0.056
	330	371	$3/2^+$	2.8 (8)	24,25	0.22	0.049
	427	648	$13/2^-$	0.33 (3)	3,4,24	0.11	0.027
	492	712	$11/2^-$	0.21 (2)	3,4,24	0.077	0.020
$^{187}\text{Au}$	323	444	$9/2^-$	0.66 (17)	30,33	0.12	0.035
	388	742	$13/2^-$	0.64 (9)	30,33	0.23	0.054
	657	881	$11/2^-$	0.10 (2)	33	0.036	0.011
$^{185}\text{Pt}$	340	521	$3/2^-$	0.35	31	0.19	0.042
	542	723	$3/2^-$	0.19	31	0.055	0.015
$^{187}\text{Pt}$	260	260	$3/2^-$	3.2 (6)	26,27	0.39	0.086
	262	288	$5/2^-$	5.7 (14)	26,27	0.38	0.084
	499	508	$3/2^-$	0.8 (3)	26,27	0.068	0.018
$^{195}\text{Pb}$	318	1126	$11/2^+$	4.9 (32)	29	0.34	0.056
	401	1177	$9/2^+$	5.4 (27)	29	0.17	0.033
$^{231}\text{Th}$	429*	634	$7/2^-$	0.66 (4)	32	0.28	0.037

\*Additional cases for  $^{231}\text{Th}$  are not shown.

The Pt isotopes are particularly interesting because they undergo a pronounced change<sup>22</sup> in their excitation spectra from higher to lower mass numbers, for example, between  $^{188}\text{Pt}$  and  $^{186}\text{Pt}$ . With regard to odd-mass Pt isotopes, a similarly drastic change occurs<sup>31,50</sup> between  $^{187}\text{Pt}$  and  $^{185}\text{Pt}$ . The  $\alpha_K > \alpha_K(\text{M1})$  transitions for these two cases are shown in fig. 4. In  $^{187}\text{Pt}$  (fig. 4a.), the states connected by the 260.5 and 262.7 keV transitions appear<sup>27</sup> to be related to the  $0^+$  ground states and  $0^+$  excited states at 472 and 798 keV respectively in  $^{186,188}\text{Pt}$  (see fig. 2). This is particularly interesting since the  $^{186}\text{Pt}$  and  $^{188}\text{Pt}$  cores are so different. In  $^{185}\text{Pt}$  (fig. 4b), a rotational band (not shown) is built on the  $9/2^+$  ground state identified as the  $9/2^+[624]$

configuration due to strong coupling between the particle and the prolate core. The states connected by the 542.2 and 340.1 keV transitions are most likely related to the coupling of the  $1/2^- [521]$  configuration to the  $0^+$  and  $0^+$  excited states in  $^{184,186}\text{Pt}$ . Previous work<sup>31</sup> on  $^{185}\text{Pt}$  indicates that the very converted transitions may be anomalous M1, like those so assigned<sup>5</sup> in  $^{185}\text{Au}$ . The evidence presented for anomalous M1 transitions in  $^{185}\text{Au}$  comes from the electron intensities assigned by Bourgeois et al.<sup>5</sup> to the 321K and 330K conversion lines. They claimed to observe  $\alpha_K > \alpha_K(\text{M1})$  for transitions between levels with different spins. We have clearly shown<sup>20</sup>, however,

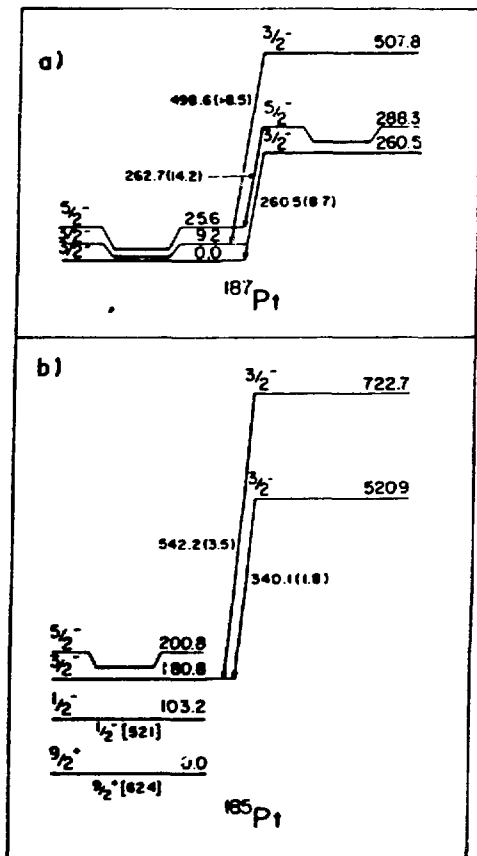


Fig. 4. Transitions in  $^{187,185}\text{Pt}$  with  $\alpha_K > \alpha_K(\text{M1})$ . All energies are in keV. The numbers in parentheses following the transition energy are the ratios  $\alpha_K(\text{expt})/\alpha_K(\text{M1 theory})$ . Data are from refs. 26,27 ( $^{187}\text{Pt}$ ) and 31,51 ( $^{185}\text{Pt}$ ).

that multiplet structure is indicated for these lines and that the very converted components occur between levels of like spin and, consequently, can carry an E0 component. Indeed, we find all transitions with  $\alpha_K > \alpha_K(\text{M1})$  in  $^{185}\text{Au}$  and  $^{187}\text{Au}$  (ref. 20) and  $^{185}\text{Pt}$  (ref. 51) to be consistent with  $\Delta I = 0$ .

Transitions with  $\alpha_K > \alpha_K(\text{M1})$  between positive parity states in  $^{185}\text{Au}$  are also observed as shown in fig. 5. The significant E0 admixture in the 330.0 and 205.2 keV transitions suggests coexisting bands for the positive parity proton-hole states ( $s_{1/2}$ ,  $d_{3/2}$ ,  $d_{5/2}$ ) in the  $^{186}\text{Hg}$  core similar to that observed for the  $h_{11/2}$  band. However, a strongly-coupled sequence of levels was observed<sup>52</sup> in-beam to feed the  $h_{11/2}$  decoupled band (no spin assignments were made in



ref. 52). This is shown in fig. 6. The cascade and crossover intraband transitions from the in-beam data clearly indicate strong-coupling. The absence of transitions indicated by dashed lines is a puzzle, but it may well be that the head of the band lies below the decay sequence of the in-beam data. Support for this interpretation comes from work<sup>53,54</sup> on  $^{187}\text{Hg}$ , but one still remains puzzled by the absence of the  $13/2^-$  level in the decay work. In this regard it should be noted that the h.c.  $13/2^-$  member at 681.1 keV lies unusually low in energy (by systematic<sup>5</sup>). This may indicate mixing of the two  $13/2^-$  states with the elusive  $13/2^-$  being repelled to a higher energy location. The lack of a clearly observable 346.3 keV transition is also part of the remaining difficulty.

We have observed<sup>24</sup> a similar strongly-coupled + decoupled sequence (via decay spectroscopy alone) for the positive parity proton-hole bands shown in fig. 7 (a continuation of fig. 5 to higher energies). Note the cascade and crossover interband transitions at higher energy. Note also the missing, but otherwise expected, transitions indicated by dashed lines. It is, therefore, not entirely certain that the 370.7, 496.3 keV levels and the 559.2, 683.0, 861.3, 1014.1 keV levels belong to the same band. This data on odd-mass core shape isomerism, represented by figs. 6 and 7, imply that the situation at low-spin is complex, probably due to mixing. This represents a new type of degree of freedom in odd-mass nuclei and needs to be clarified in  $^{185}\text{Au}$  and searched for in other nuclei.

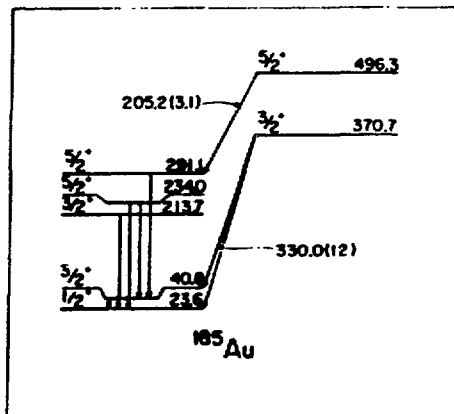


Fig. 5. Transitions with  $\alpha_K > \alpha_K(\text{M1})$  between positive parity states in  $^{185}\text{Au}$ . All energies are in keV. The numbers in parentheses following the transition energy are the ratios  $\alpha_K(\text{expt})/\alpha_K(\text{M1 theory})$ . Data are from ref. 24.

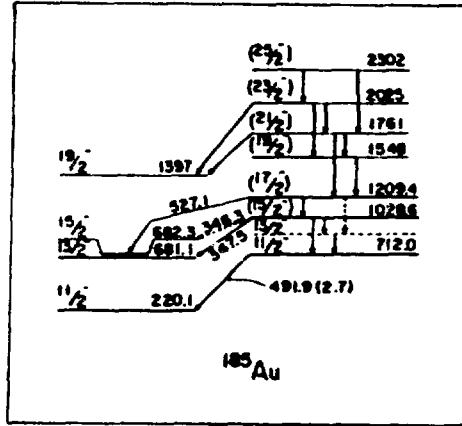


Fig. 6. Portions of the  $h_{11/2}$  structure in  $^{185}\text{Au}$  as seen in decay and in-beam spectroscopy. The  $11/2^-$  [220 keV],  $15/2^-$  [682 keV] and  $11/2^-$  [712 keV], ( $15/2^-$ ) [1029 keV] levels and the 491.9 keV transition were shown earlier in fig. 1b. All energies are in keV. The levels and transitions with energies to 0.1 keV are seen in decay spectroscopy (ref. 24). The upper levels with energies to 1 keV are seen only in in-beam spectroscopy (ref. 52). The 1209.4, 682.3 and 220.1 keV levels and the 527.1 keV transition are seen both in-beam<sup>52</sup> and in the  $^{185}\text{m}, ^{185}\text{gHg}$  decay<sup>24</sup>.

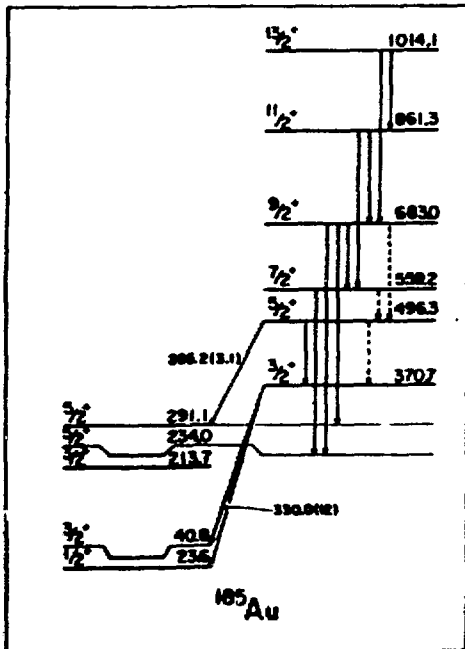


Fig. 7. Possible continuation of the upper positive parity band in  $^{185}\text{Au}$  shown in fig. 5 (370.7 and 496.3 keV). All energies are in keV and other notations are as indicated for fig. 5. Data are from ref. 20.

### CONCLUSIONS AND FUTURE

Recent work bearing on the data presented here include the observation<sup>55</sup> of a very large isotope shift,  $\delta\langle r^2 \rangle$ , between  $^{187}\text{Au}$  and  $^{186}\text{Au}$  ( $\beta = 0.25$  for  $^{185,186}\text{Au}$ ); the extension of the Hg isotope shift data to  $^{182}\text{Hg}$  and the observation of the  $^{185}\text{mHg}/^{185}\text{gHg}$  isomer shift (the largest isotope/isomer shifts known anywhere -- see ref. 56);

13. J. D. Cole et al., Phys. Rev. C16, 2010 (1977).
14. J. D. Cole et al., Phys. Rev. C30, 1267 (1984).
15. W. C. Ma et al., Phys. Lett. B139, 276 (1984).
16. K. Heyde et al., Nucl. Phys. A466, 189 (1987).
17. K. Heyde, contribution to this conference.
18. J. L. Wood, contribution to this conference.
19. P. Van Duppen et al., Phys. Rev. C35, 1861 (1987).
20. C. D. Papanicolopoulos et al., Phys. Lett. B, preprint.
21. M. Cailliau et al., J. de Phys. 35, 469 (1974).
22. M. Finger et al., Nucl. Phys. A188, 369 (1972).
23. F. Rosel et al., At. Data Nucl. Data Tables 21, 291 (1978).
24. C. D. Papanicolopoulos, Ph.D. thesis, Ga. Tech., 1987.
25. C. D. Papanicolopoulos et al., Contribution to this Conference.
26. A. Ben Braham et al., Nucl. Phys. A332, 397 (1979).
27. B. E. Gnade et al., Nucl. Phys. A406, 29 (1983).
28. M. I. Macias-Marques et al., Nucl. Phys. A427, 205 (1984).
29. J. C. Griffin, Ph.D. thesis, Ga. Tech., 1987.
30. E. F. Zganjar et al., in Proc. 4th Int. Conf. on Nuclei Far From Stability, Helsingør, Denmark, 1981, ed. P. G. Hansen and O. B. Nielsen, CERN Report 81-09, p. 630.
31. B. Roussiere et al., Nucl. Phys. A438, 93 (1985).
32. D. H. White et al., Phys. Rev. C35, 81 (1987).
33. M. A. Grimm, Ph.D. thesis, Ga. Tech., 1978.
34. F. Schussler et al., Nucl. Phys. A339, 415 (1980).
35. T. A. Khan et al., Nucl. Phys. A283, 105 (1977).
36. J. D. Cole, Ph.D. thesis, Vanderbilt, 1978.
37. C. M. Baglin, Nucl. Data Sheets 30, 1 (1980).
38. Y. A. Ellis-Akovali, Nucl. Data Sheets 40, 385 (1983).
39. E. Hagberg et al., Nucl. Phys. A318, 29 (1979).
40. J. P. Husson et al., in Proc. Third Int. Conf. on Nuclei Far From Stability, Cargese, 1976, ed. R. Klapisch, CERN 76-13, p. 460.
41. P. T. Prokofjev et al., Nucl. Phys. A455, 1 (1986).
42. E. G. Funk et al., Phys. Rev. C10, 2015 (1974).
43. T. von Egidy et al., Phys. Lett. 81B, 281 (1979).
44. W. Z. Venema et al., Phys. Lett. 156B, 163 (1985).
45. J. Almeida et al., Nucl. Phys. A315, 71 (1979).
46. G. M. Gowdy, Ph.D. thesis, Ga. Tech., 1976.
47. G. M. Gowdy et al., Nucl. Phys. A312, 56 (1978).
48. R. A. Braga et al., Phys. Rev. C19, 2305 (1979).
49. C. R. Bingham, private communication.
50. J. L. Wood, in proc. 4th Int. Conf. on Nuclei Far From Stability, Helsingør, Denmark, 1981, ed. P. G. Hansen and O. B. Nielsen, CERN Report 81-09, p. 612.
51. J. Schwarzenberg, Ga. Tech., private communication.
52. A. J. Larabee et al., Phys. Lett. 169B, 21 (1986).
53. J. L. Wood et al., Bull. Am. Phys. Soc. 25, 739 (1980).
54. F. Hannachi et al., Z. Phys. A325, 371 (1986).
55. K. Wallmeroth et al., Phys. Rev. Lett. 58, 1516 (1987).
56. G. Ulm et al., Z. Phys. A325, 247 (1986).
57. F. Hannachi et al., Z. Phys. A325, 371 (1986).
58. G. D. Dracoulis et al., J. Phys. G12, L97 (1986).
59. J. Kantele et al., Phys. Rev. Lett. 51, 91 (1983).
60. J. Lange et al., Rev. Mod. Phys. 54, 119 (1982).